

**Alignment-assisted field-free orientation of rotationally cold CO molecules**Xiaoming Ren,<sup>1</sup> Varun Makhija,<sup>1</sup> Hui Li,<sup>1</sup> Matthias F. Kling,<sup>1,2</sup> and Vinod Kumarappan<sup>1,\*</sup><sup>1</sup>*James R. Macdonald Laboratory, Kansas State University, Manhattan, Kansas 66506, USA*<sup>2</sup>*Max Planck Institute of Quantum Optics, Hans-Kopfermann-Strasse 1, D-85748 Garching, Germany*

(Received 16 June 2014; published 25 July 2014)

We follow the alignment-assisted orientation technique proposed by Zhang *et al.* [*Phys. Rev. A* **83**, 043410 (2011)] to experimentally demonstrate a substantial enhancement of the field-free orientation by using a combination of single- and two-color laser pulses. When a two-color orienting pulse is preceded by a single-color aligning pulse by a suitable time, the resulting orientation is thrice as large as that obtained with the two-color pulse alone. We ensure that the orientation is the result of the hyperpolarizability interaction rather than ionization depletion by keeping the ionization due to the pump pulses small and demonstrate a useful level of orientation without the complications of a partially ionized target.

DOI: [10.1103/PhysRevA.90.013419](https://doi.org/10.1103/PhysRevA.90.013419)

PACS number(s): 37.10.Vz, 33.15.Bh, 42.50.Hz, 42.65.Re

**I. INTRODUCTION**

Molecular alignment using nonresonant laser pulses [1–5] has been intensively studied in the last two decades. By confining the distribution of molecular axes to laboratory axes, laser-induced alignment makes measurements in the molecular frame accessible and has enabled, for instance, unprecedented information and resolution about the molecular structure [6–8] and allowing angle-resolved measurements to be made when the molecules interact with an external field [9–11]. But alignment is sufficient for molecular frame measurements only if the molecule has a mirror plane perpendicular to the axis. This is the case, for instance, for the nitrogen molecule, in which the two atoms are indistinguishable and the N-N bond is not directed. For molecules such as carbon monoxide, the atoms are distinguishable and the molecular axis is a directed line. Thus, it becomes necessary to apply external fields that also lack reflection symmetry and orient the molecules by forcing the carbon atoms to point in one direction and the oxygen atoms in the opposite direction. Nonoptical techniques such as hexapole focusing [12] and brute force [13] were developed to achieve molecular orientation. The first method uses state selection in a hexapole lens followed by a uniform static field and results in an oriented ensemble with very low gas density. The second method requires—as its name implies—strong static fields to achieve a reasonable degree of orientation. As a more widely applicable technique, laser-induced molecular orientation was first proposed [14,15] and demonstrated [16,17] by using a combination of an adiabatic nonresonant laser field and an electrostatic field. Even though it yields a high degree of orientation, especially with rotationally cold targets, it fails to produce orientation under field-free conditions. At the cost of significant experimental effort, the orientation can be made laser-field free by using a combination of the electrostatic field with a slow-turn-on and rapid-turn-off field [18] or with an intense ultrashort nonresonant laser field [19]. To achieve field-free orientation, two techniques have been proposed. One is to use terahertz pulses [20–24] and the other uses two-color pulses [25–27]. The basic principle in both cases is the same—making the driving field asymmetric.

The former uses single or half-cycle terahertz pulses to reduce cycle averaging on the dipole interaction. Experiments have been reported on orienting room-temperature OCS molecules [22] and rotationally cooled HBr molecules [23], but both achieve a rather weak degree of orientation.

The two-color field-free orientation method uses overlapping and phase-locked fundamental and second-harmonic pulses. There are two possible mechanisms for producing orientation when the field interacts with the molecules. In the first mechanism, the field selectively ionizes molecules oriented in one direction and depletes the population of neutral molecules in that orientation. The neutral molecules that remain after the pulse are, therefore, oriented [28–30]. But this leaves behind a mixture of neutral molecules—perhaps in excited states—and ions that may be an unsuitable target for further measurements. In the second mechanism, the pulse interacts with the molecule’s hyperpolarizability tensor and torques the molecules into orientation. The relative contributions of these two mechanisms depends on the intensity of the two-color pulse, with the hyperpolarizability interaction dominant at low intensities and ionization depletion taking over once significant ionization sets in.

Since molecules with high ionization potentials are usually weakly hyperpolarizable, the degree of orientation using the hyperpolarizability interaction alone tends to be low [28]. Since the first experimental demonstration of this technique [27], various approaches to increase the degree of orientation—for instance, by using two time-separated two-color fields [31], or a combination of single- and two-color fields [32]—have been proposed. The former provides control of the rotational wave packet and enhances the orientation by a factor of two. The latter has been shown computationally to be very efficient for orienting molecules at both low [33] and high [34] rotational temperatures. In simulations, a three-fold enhancement in orientation can be obtained when the single-color field is positioned correctly with respect to the two-color field [33,34]. In this article, we report the experimental demonstration of this technique using only the hyperpolarizability mechanism in CO. By applying an aligning pulse before the orienting two-color pulse, the degree of orientation [characterized by  $\langle \cos \theta_{2D} \rangle$ , where  $\theta_{2D}$  is the angle between the laser polarization axis and the projection of the  $C^{2+}$  fragment’s momentum vector measured by using a

\*vinod@phys.ksu.edu

velocity map imaging (VMI) spectrometer [35] is increased from 0.07 to 0.2 in rotationally cold CO molecules.

## II. ORIENTATION BY HYPERPOLARIZABILITY INTERACTION

The electric field of a two-color pulse comprising pulses at the fundamental frequency  $\omega$  and the second harmonic  $2\omega$  can be expressed as  $E(t) = \varepsilon_\omega(t)e^{i\omega t} + \varepsilon_{2\omega}(t)e^{i2\omega t + \varphi}$ , where  $\varepsilon_\omega$  and  $\varepsilon_{2\omega}$  are amplitudes of the individual fields and  $\varphi$  is the relative phase. Including the dipole, the polarizability and the hyperpolarizability interaction terms, the rotational Hamiltonian for a linear molecule lacking inversion symmetry in such a field is [33]

$$H = BJ^2 - \mu E(t) \cos \theta - \frac{1}{2}[(\alpha_{\parallel} - \alpha_{\perp}) \cos^2 \theta + \alpha_{\perp}]E(t)^2 - \frac{1}{6}[(\beta_{\parallel} - 3\beta_{\perp}) \cos^3 \theta + 3\beta_{\perp} \cos \theta]E(t)^3, \quad (1)$$

where  $B$  is the rotational constant of the molecule,  $J$  is the total angular momentum,  $\mu$  is the dipole moment, and  $\alpha_{\parallel}$  ( $\beta_{\parallel}$ ) and  $\alpha_{\perp}$  ( $\beta_{\perp}$ ) are the parallel and perpendicular components of the polarizability (hyperpolarizability) tensor, respectively [36]. After cycle averaging over the fundamental optical field, the effective Hamiltonian is [33]

$$\bar{H} = BJ^2 - \frac{1}{4}[(\alpha_{\parallel} - \alpha_{\perp}) \cos^2 \theta + \alpha_{\perp}][\varepsilon_\omega^2(t) + \varepsilon_{2\omega}^2(t)] - \frac{1}{8}[(\beta_{\parallel} - 3\beta_{\perp}) \cos^3 \theta + 3\beta_{\perp} \cos \theta]\varepsilon_\omega^2(t)\varepsilon_{2\omega}(t) \cos \varphi. \quad (2)$$

By solving the time-dependent Schrödinger equation (TDSE) with this Hamiltonian, the evolution of both alignment and orientation—characterized by  $\langle \cos^2 \theta \rangle$  and  $\langle \cos \theta \rangle$ , respectively, can be calculated for any initial rotational state. These expectation values are

$$\langle \cos^n \theta \rangle(t) = \sum_{J,J'} C_{JM}^* C_{J'M} e^{-i(E_{J'} - E_J)t} \langle JM | \cos^n \theta | J'M \rangle, \quad (3)$$

where  $n = 1, 2$ ;  $J, J'$  are total angular momentum quantum numbers;  $|JM\rangle$  is the eigenstate of the field-free rotational Hamiltonian;  $C_{JM}$  are coefficients of the  $|JM\rangle$  component of the field-free rotational wave packet;  $E_J$  is the energy of the  $|JM\rangle$  eigenstate. Note that, in terms of the fundamental rotation period  $T$  of the molecule,  $E_J = J(J+1)/(2T)$ .

As pointed out by Zhang *et al.* [32], a consequence of this expression is that the orientations of rotational wave packets produced from even and odd initial  $J$  states have opposite signs at  $T/2$ . Therefore, a gas with equal populations in initial states of the two parities exhibits no orientation at half the rotational period. This phenomenon is akin to the well-known presence of full-strength quarter revivals in the alignment of oxygen, which has no even- $J$  states populated due to nuclear-spin statistics, and only partial quarter revivals in nitrogen, which has a 1 : 2 ratio of even- and odd- $J$  states populated. In the case of CO, no half revivals of orientation are expected

when the rotational temperature of the gas is high enough. We will show experimental evidence of such revivals when the molecular rotational temperature is low and, consequently, the two initial populations are not equal.

The cancellation of orientation at the half revivals is unfortunate—calculations by Zhang *et al.* [32] show that both even- and odd- $J$  states taken separately are much better oriented at the half revival than at the full revival [see Fig. 5(b)]. Therefore, if one can manipulate the evolution of the even- and odd- $J$  states so that the strong orientation peaks match up in phase or even eliminate one parity of the  $J$  state, the degree of orientation will be greatly enhanced. To achieve this, Zhang *et al.* proposed alignment-assisted orientation: arriving a quarter (or three quarters) of a rotational period after a single-color alignment pulse, the two-color orientation pulse enhances the orientation of one parity while destroying the wave packet of the other parity. This is reminiscent of phase control of rotational wave packets by Lee *et al.* [37], where a similar scheme was used either to turn off the alignment revivals completely or to double the periodicity of the revivals by applying a second pulse at the quarter revival.

## III. ORIENTATION BY TWO-COLOR PULSE

Our experimental setup is shown in Fig. 1. The output of the Kansas Light Source—an 800 nm, 30 fs, 2 mJ, 2 kHz laser system—is split into pump and probe arms using a broadband 80/20 beam splitter. The 20% beam goes to the probe arm and is focused into the VMI spectrometer by using a 25 cm

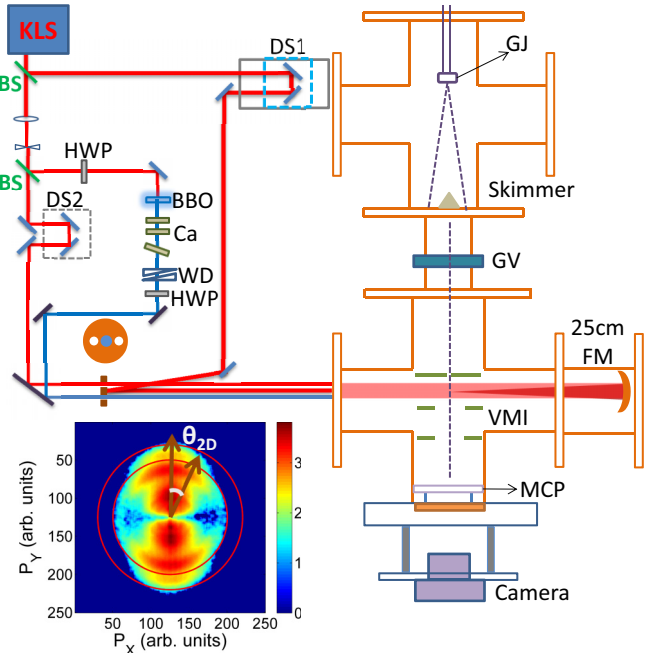


FIG. 1. (Color online) Experimental setup. KLS: Kansas Light Source; BS: beam splitter; HWP: half-wave plate; MCP: microchannel plate; DS1 and DS2: delay stages; Ca: calcite; WD: wedge pair; GJ: gas jet; GV: gate valve; FM: focusing mirror. A two-dimensional momentum distribution of the  $C^{2+}$  ion is shown at the bottom. The circles indicate the region at which the  $\langle \cos \theta_{2D} \rangle$  and  $\langle \cos^2 \theta_{2D} \rangle$  are measured. See text for other experimental details.

focusing mirror. The rest goes to the pump arm in which a telescope is used to reduce the beam size by a factor of two in order to increase the efficiency of second-harmonic generation as well as reducing the intensity of the pump pulses at the focus so that they do not ionize the molecules. After the telescope, this beam is split again by a 70/30 beam splitter, 70% goes through a type-I, 200- $\mu\text{m}$ -thick BBO crystal to generate the second harmonic. Three 600- $\mu\text{m}$ -thick calcite plates and a pair of wedges are used to compensate the delay between the fundamental and its second harmonic introduced in the crystal and entrance window of the chamber. One of the calcite plates is mounted on a motorized rotational stage to control the relative phase  $\varphi$ . The two-color beam then recombines with the 30% single-color beam and the probe beam on a mirror with two holes and all beams are focused together into the target gas by the same focusing mirror. A 20% mixture of CO in helium (500 psi total pressure) is cooled to  $\sim 3$  K by supersonic expansion using a kHz Even–Lavie valve [38], and the central part of the jet is skimmed into the VMI chamber. In the interaction region, the pumps align and orient the CO molecules, the probe Coulomb explodes the molecules and the momentum distribution of the fragments are recorded for every other laser shot by a microchannel plate (MCP), a fast phosphor screen and a 1000-frames-per-second CMOS camera at every pump-probe delay. In order to make the most direct comparison with previous measurements [27], the momentum distribution images from the  $\text{C}^{2+}$  fragment are recorded and used to calculate the  $\langle \cos \theta_{2D} \rangle$  and  $\langle \cos^2 \theta_{2D} \rangle$  traces by gating on the channel with the highest kinetic energy (see Fig. 1). Since we account for probe selectivity (see below), the influence of choosing this particular channel is largely accounted for and we expect that similar results will be obtained if other Coulomb explosion channels were to be used for characterizing the orientation. The pump-probe delay dependence of both with only the two-color pump are shown in Fig. 2 for  $\varphi = 0$  and  $\pi$ .

Maximum orientation is achieved at about 3.8 ps, which is close to half the rotational period, with  $\langle \cos \theta_{2D} \rangle \simeq 0.07$ . Two important features are noteworthy. First, the peak of the orientation near the full revival ( $\sim 8.2$  ps) is slightly before the peak of the anti-alignment ( $\sim 8.4$  ps), indicating that the orientation is due to the hyperpolarizability interaction rather than ionization depletion [28]. Second, alignment and orientation peaks at one fourth and one half of the rotational period, respectively. Especially for the orientation, the peak at the half revival is even higher than the one at the full revival. These features were not observed in Ref. [27], where the rotational temperature was estimated to be 60 K. At this temperature, the thermal population of even- and odd- $J$  states is equal. As discussed previously,  $\langle \cos^2 \theta \rangle$  and  $\langle \cos \theta \rangle$  calculated from those even- and odd-initial- $J$  states have a  $\pi$  phase difference at the quarter and half revivals and alignment and orientation at those revivals cancel out. However, if the temperature is very low, few  $J$  states are populated and the populations in even- and odd- $J$  states are not the same. This results in appreciable recurrence of alignment at the quarter revival and of orientation at the half revival. Furthermore, for CO calculations show comparable degrees of orientation at the half and full revivals only when the rotational temperature is below 5 K. In our case a rotational temperature of 3 K yields the best agreement between calculation and experiment.

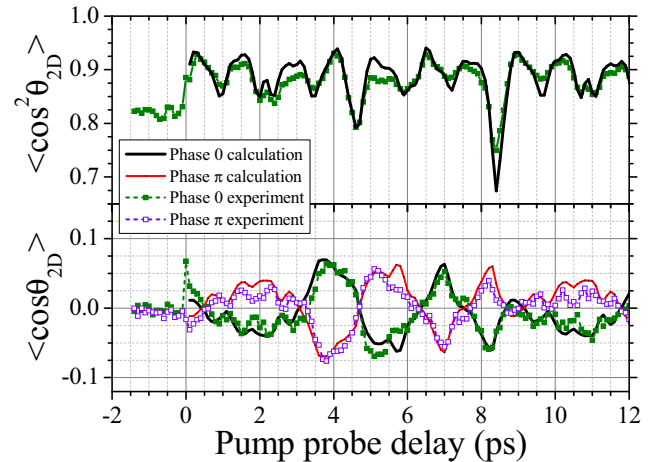


FIG. 2. (Color online) Measured and calculated values of  $\langle \cos \theta_{2D} \rangle$  and  $\langle \cos^2 \theta_{2D} \rangle$  with only the two-color pump. The calculations are performed on the two-dimensional projection of the calculated three-dimensional angular distribution convolved with the probe selectivity. The duration of the pump pulse was measured to be 70 fs for the red (800 nm) part of the two-color pulse, the blue (400 nm) part is assumed to have the same pulse duration. The total intensity is estimated to be 52 TW/cm<sup>2</sup> with a blue-to-red intensity ratio of three. The molecular rotational temperature is estimated to be 3 K.

In order to simulate the experimental results, two factors are taken into account. First,  $\langle \cos \theta_{2D} \rangle$  is measured, while  $\langle \cos \theta \rangle$  is calculated from the TDSE. Second, the likelihood of the probe pulse producing a  $\text{C}^{2+}$  ion depends on the angle between the molecular axis and the probe polarization. Even without the pump beams, the  $\langle \cos^2 \theta_{2D} \rangle$  is measured to be much higher than the isotropic two-dimensional (2D) value 0.5 because the probe beam preferentially ionizes molecules that lie along its polarization direction. To calculate the 2D value, we solve the TDSE to get the angular probability distribution  $\rho(\theta, \phi)$  at each time delay, where  $\phi$  is the azimuthal angle around the laser polarization axis. Note that there is no  $\phi$  dependence because the interaction with the driving field has cylindrical symmetry. To account for probe selectivity, a probe-only image with high statistics is measured and inverted by using an iterative procedure [39]. The same kinetic-energy channel is then gated on the inverted image to obtain the probe selectivity  $P(\theta)$  for that particular channel. Furthermore, since  $P(\theta = 90^\circ)$  cannot be precisely determined due to the lack of statistics and presence of background noise at that angle, a constant offset  $\delta$  is subtracted from  $P(\theta)$  and the selectivity is then renormalized. This corrected selectivity function is convolved with the calculated three-dimensional (3D) distribution and the final  $\langle \cos^2 \theta_{2D} \rangle$  and  $\langle \cos \theta_{2D} \rangle$  values are calculated on the 2D projections of  $\rho(\theta, \phi)P(\theta)$ . A table of different  $\delta$  values, rotational temperatures, and total intensities of the two-color pulse is used to find the least-square error between the experiment and calculation. The optimum solutions are plotted as solid curves in Fig. 2 for both  $\varphi = 0$  and  $\pi$ . The structures and magnitudes of both alignment and orientation traces show good agreement between the calculations and measurements.

#### IV. ALIGNMENT-ASSISTED ORIENTATION

The next step is to position the single-color pump before the two-color pump. The optimum separation between the two pumps has been estimated to be around 1/4 or 3/4 of the rotational period [33,34]. However, this number varies with different rotational temperatures and laser parameters, especially for positioning the two-color pump at the 1/4 revival due to the single-color pump [34]. Our calculations show that the optimum separation changes from 1/5 of the rotational period at 3 K to 1/4 at 30 K. But when positioning at the 3/4 revival, this value does not vary much with temperature and is less sensitive to the time separations of the two pumps. Therefore, experimentally, we choose a separation of about 6.48 ps. Alignment and orientation traces are recorded and shown in the scatter plots of Fig. 3 for both  $\varphi = 0$  and  $\pi$  along with the calculated values of  $\langle \cos^2 \theta_{2D} \rangle$  and  $\langle \cos \theta_{2D} \rangle$  with probe selectivity. Again, a table of different single-color pulse intensities is used to find this optimum solution. The maximum  $\langle \cos \theta_{2D} \rangle$  obtained in the experiment is  $\sim 0.2$ , which is reached at a delay of 11.1 ps with respect to the single-color pump. The overall agreement of the revival structure is good except for the differences in magnitude at the peak of the orientation. Further calculations were attempted to match the peak magnitudes, but the agreement of the structures degraded elsewhere. This may be attributable to the lack of intensity averaging in the calculation.

Momentum distributions with no pumps and at the peak orientation with the two-color pump alone and with both pumps were also measured with high statistics. These images were Abel inverted and the center slices are shown in Fig. 4. A substantial increment of asymmetry can be seen from the images, indicating enhancement of orientation. The measured  $\langle \cos \theta \rangle_m$  (the subscript m stands for ‘‘measured,’’ without correction for probe selectivity) values from those images are 0, 0.064, and 0.194, respectively. Compared with the value of

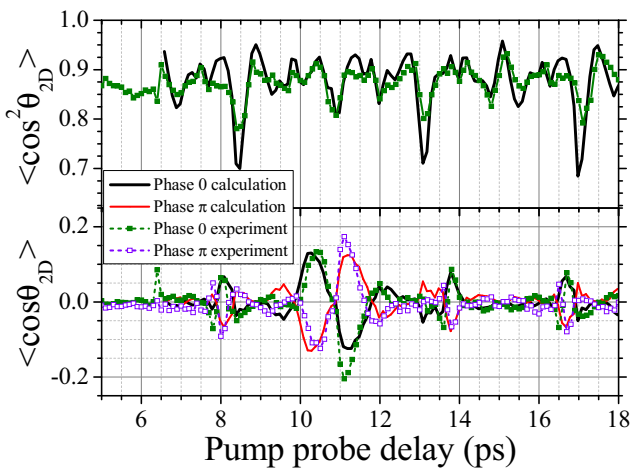


FIG. 3. (Color online) Experimental measurements and calculations of  $\langle \cos \theta_{2D} \rangle$  and  $\langle \cos^2 \theta_{2D} \rangle$  with both single-color and the two-color pulses. The same image processing is performed as in the two-color only case. The two-color pulse parameters are the same as shown in Fig. 2 and the parameters for the single-color pulse are 85 fs and 42 TW/cm<sup>2</sup>.

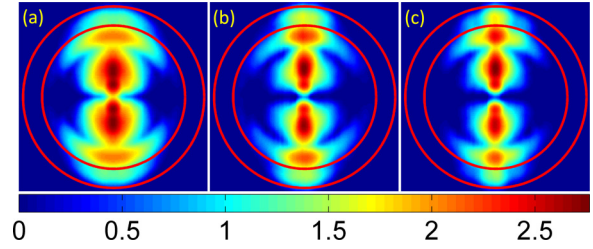


FIG. 4. (Color online) Image (a) shows the momentum distribution with no orientation. Images (b) and (c) show the momentum distribution at the peak orientation with the two-color-only pump and both pumps, respectively. All the images were Gauss smoothed and then Abel inverted. Note that the color scale is logarithmic.

0.06 previously reported [27,30] for the same variable, we have achieved a much better degree of orientation while remaining in the hyperpolarizability regime.

Calculated  $\langle \cos^2 \theta \rangle$  and  $\langle \cos \theta \rangle$  traces without the probe selectivity are plotted in Fig. 5 by using the retrieved laser parameters. According to the calculation, the actual degree of orientation is about 0.04 for the two-color only case, which increases to 0.11 by adding the aligning pulse. We note that both 2D projection and probe selectivity cause the measured orientation level  $\langle \cos \theta_{2D} \rangle$  to be higher than the actual level  $\langle \cos \theta \rangle$ . This has not been taken into account in previous work.

In order to show the mechanism of the alignment-assisted orientation technique as discussed in the introduction, the orientation traces for even- and odd- $J$  initial states are plotted separately for both the two-color only case and the alignment-assisted case. As shown in Fig. 5(b), with only the two-color pulse both even- and odd- $J$  states individually are strongly oriented at the half revival ( $\sim 4$  ps) but are out of phase, resulting in weak net orientation or even no orientation when the temperature is higher. At the full revival, although even- and odd- $J$  states are in phase, they are both only weakly oriented and the sum of the two is still small. This explains why the hyperpolarizability interaction tends to result in very

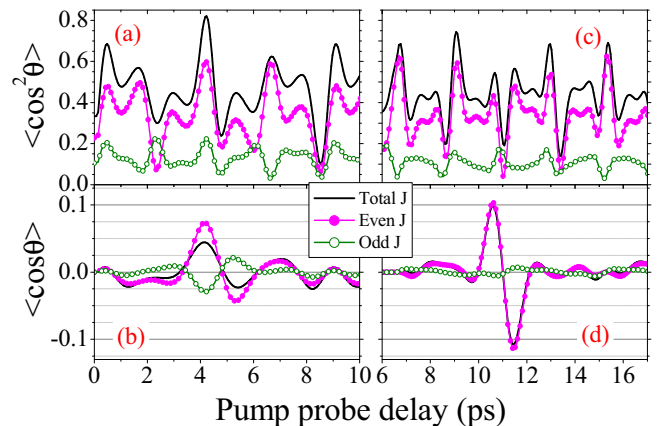


FIG. 5. (Color online) Calculation of the alignment and orientation trace for the two-color-only pump [panels (a) and (b)] and both pumps [panels (c) and (d)]. The time evolution of orientation from even- and odd- $J$  states are also plotted separately. Rotational temperature and laser parameters are all the same as before.

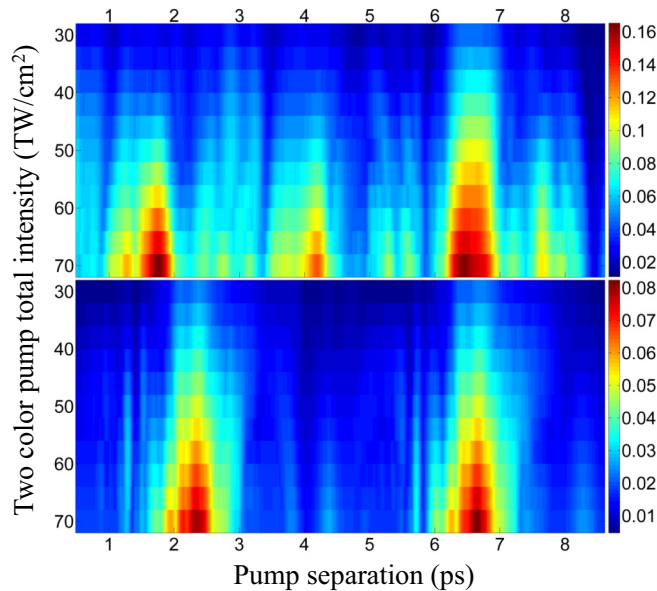


FIG. 6. (Color online) Top graph: The maximum  $\langle \cos \theta \rangle$  values calculated for each combination from a table of pump separations and two color total intensities at 3 K, pump separation goes from 0.5 to 8.6 ps with a step size of 0.1 ps, two-color total intensity changes from 30 to 70  $\text{TW}/\text{cm}^2$  with a step size of 2  $\text{TW}/\text{cm}^2$ . Bottom graph: the same calculation for a rotational temperature of 30 K.

weak orientation with just the two-color pulse. However, by adding an extra aligning pulse, as described previously, the evolution of the even- and odd- $J$  states can be manipulated differently to enhance the degree of orientation. In our case, at the optimum separation, as shown in Fig. 5(d), the orientation from even- $J$  states gets enhanced, while the overall modulation in the orientation from odd- $J$  states is diminished. Therefore, the resulting orientation trace follows the even- $J$  states and results in much stronger net orientation at the half revival after the two-color pulse.

Although the degree of orientation we obtain is relatively high, it can be further enhanced with a higher-energy two-color pulse without significant ionization. Figure 6 shows the effectiveness of this technique. In the top graph, all the other experimental conditions are fixed except for the total two-color intensity and the pump separation. The maximum  $\langle \cos \theta \rangle$  values are calculated and plotted at each combination of the two. The overall maximum is above 0.16 at the highest total intensity of 70  $\text{TW}/\text{cm}^2$ , estimated to be the highest two-color intensity at which the ionization can still be neglected [28]. Furthermore, if the two-color pulse duration can be stretched to increase the fluence while maintaining low levels of ionization, the degree of orientation can be further enhanced [33].

However, practically, care needs to be taken to stretch the pulse durations while maintaining a reasonable blue-to-red ratio in the two-color beam. The good degree of orientation we have achieved is also a product of the low rotational temperature provided by our jet. Such low temperatures are not practical for all experiments. For instance, high harmonic generation [29] requires higher gas density and, when a jet is used, is normally performed at the exit of the nozzle. In this case, even with the Even-Lavie valve, the rotational temperature will be substantially higher. To test the effectiveness of alignment-assisted orientation, a similar calculation is also carried out and shown in the bottom graph of Fig. 6, which demonstrates that a reasonable degree of orientation is also achievable at higher temperature.

## V. CONCLUSION

In conclusion, we have successfully demonstrated the alignment-assisted field-free orientation technique experimentally by using a combination of single- and two-color laser field. By using rotationally cold CO molecules, the degree of orientation is increased by about a factor of three compared to a single two-color pulse. Care was taken to ensure that ionization depletion did not play a role in the experiment; the orientation was obtained by using the hyperpolarizability interaction. This is important for experiments where ionization from the pump pulses would be a significant impediment. We also note that this technique is not limited to using the two-color field; alignment-assisted field-free orientation using a THz pulse has been demonstrated recently [24] and has shown substantially better orientation. Therefore the technique is general and very efficient. We expect it to provide oriented gas samples for the study of molecular structures and dynamics. Although the degree of orientation is not very large, it is expected to be sufficient for experiments that produce no signal in the absence of orientation. The generation of even-order harmonics [29], and measurements of up-down asymmetry in electron momentum spectra are two important examples. Experiments that can tolerate some ionization by the two-color pulse can benefit from better orientation through the ionization depletion mechanism.

## ACKNOWLEDGMENTS

This work is supported by Chemical Sciences, Geosciences, and Biosciences Division, Office of Basic Energy Science, Office of Science, US Department of Energy. M.F.K acknowledges support by the DFG through the cluster of excellence “Munich Centre for Advanced Photonics (MAP).”

- [1] T. Seideman, *J. Chem. Phys.* **103**, 7887 (1995).
- [2] B. Friedrich and D. Herschbach, *Phys. Rev. Lett.* **74**, 4623 (1995).
- [3] D. Normand, L. A. Lompre, and C. Cornaggia, *J. Phys. B: At., Mol. Opt. Phys.* **25**, L497 (1992).

- [4] T. Seideman, *Phys. Rev. Lett.* **83**, 4971 (1999).
- [5] F. Rosca-Pruna and M. J. J. Vrakking, *Phys. Rev. Lett.* **87**, 153902 (2001).
- [6] J. Itatani, J. Levesque, D. Zeidler, H. Niikura, H. Pépin, J.-C. Kieffer, P. B. Corkum, and D. M. Villeneuve, *Nature (London)* **432**, 867 (2004).

- [7] C. Vozzi, M. Negro, F. Calegari, G. Sansone, M. Nisoli, S. De Silvestri, and S. Stagira, *Nat. Phys.* **7**, 822 (2011).
- [8] C. J. Hensley, J. Yang, and M. Centurion, *Phys. Rev. Lett.* **109**, 133202 (2012).
- [9] V. Kumarappan, L. Holmegaard, C. Martiny, C. B. Madsen, T. K. Kjeldsen, S. S. Viftrup, L. B. Madsen, and H. Stapelfeldt, *Phys. Rev. Lett.* **100**, 093006 (2008).
- [10] D. Pavičić, K. F. Lee, D. M. Rayner, P. B. Corkum, and D. M. Villeneuve, *Phys. Rev. Lett.* **98**, 243001 (2007).
- [11] X. Ren, V. Makhija, A.-T. Le, J. Troß, S. Mondal, C. Jin, V. Kumarappan, and C. Trallero-Herrero, *Phys. Rev. A* **88**, 043421 (2013).
- [12] K. H. Kramer and R. B. Bernstein, *J. Chem. Phys.* **42**, 767 (1965).
- [13] H. J. Loesch and A. Remscheid, *J. Chem. Phys.* **93**, 4779 (1990).
- [14] B. Friedrich and D. Herschbach, *J. Chem. Phys.* **111**, 6157 (1999).
- [15] L. Cai, J. Marango, and B. Friedrich, *Phys. Rev. Lett.* **86**, 775 (2001).
- [16] H. Sakai, S. Minemoto, H. Nanjo, H. Tanji, and T. Suzuki, *Phys. Rev. Lett.* **90**, 083001 (2003).
- [17] L. Holmegaard, J. H. Nielsen, I. Nevo, H. Stapelfeldt, F. Filsinger, J. Küpper, and G. Meijer, *Phys. Rev. Lett.* **102**, 023001 (2009).
- [18] Y. Sugawara, A. Goban, S. Minemoto, and H. Sakai, *Phys. Rev. A* **77**, 031403 (2008).
- [19] O. Ghafur, A. Rouzée, A. Gijbetsen, W. K. Siu, S. Stolte, and M. J. Vrakking, *Nat. Phys.* **5**, 289 (2009).
- [20] M. Machholm and N. E. Henriksen, *Phys. Rev. Lett.* **87**, 193001 (2001).
- [21] C. Qin, Y. Tang, Y. Wang, and B. Zhang, *Phys. Rev. A* **85**, 053415 (2012).
- [22] S. Fleischer, Y. Zhou, R. W. Field, and K. A. Nelson, *Phys. Rev. Lett.* **107**, 163603 (2011).
- [23] K. Kitano, N. Ishii, N. Kanda, Y. Matsumoto, T. Kanai, M. Kuwata-Gonokami, and J. Itatani, *Phys. Rev. A* **88**, 061405 (2013).
- [24] K. N. Egodapitiya, S. Li, and R. R. Jones, *Phys. Rev. Lett.* **112**, 103002 (2014).
- [25] T. Kanai and H. Sakai, *J. Chem. Phys.* **115**, 5492 (2001).
- [26] R. Tehini and D. Sugny, *Phys. Rev. A* **77**, 023407 (2008).
- [27] S. De, I. Znakovskaya, D. Ray, F. Anis, N. G. Johnson, I. A. Bocharova, M. Magrakvelidze, B. D. Esry, C. L. Cocke, I. V. Litvinyuk, and M. F. Kling, *Phys. Rev. Lett.* **103**, 153002 (2009).
- [28] M. Spanner, S. Patchkovskii, E. Frumker, and P. Corkum, *Phys. Rev. Lett.* **109**, 113001 (2012).
- [29] E. Frumker, C. T. Hebeisen, N. Kajumba, J. B. Bertrand, H. J. Wörner, M. Spanner, D. M. Villeneuve, A. Naumov, and P. B. Corkum, *Phys. Rev. Lett.* **109**, 113901 (2012).
- [30] I. Znakovskaya, M. Spanner, S. De, H. Li, D. Ray, P. Corkum, I. V. Litvinyuk, C. L. Cocke, and M. F. Kling, *Phys. Rev. Lett.* **112**, 113005 (2014).
- [31] J. Wu and H. Zeng, *Phys. Rev. A* **81**, 053401 (2010).
- [32] S. Zhang, C. Lu, T. Jia, Z. Wang, and Z. Sun, *Phys. Rev. A* **83**, 043410 (2011).
- [33] K. Nakajima, H. Abe, and Y. Ohtsuki, *J. Phys. Chem. A* **116**, 11219 (2012).
- [34] R. Tehini, M. Z. Hoque, O. Faucher, and D. Sugny, *Phys. Rev. A* **85**, 043423 (2012).
- [35] A. T. Eppink and D. H. Parker, *Rev. Sci. Instrum.* **68**, 3477 (1997).
- [36] For CO,  $B = 1.93128 \text{ cm}^{-1}$ , and (in atomic units)  $\alpha_{\parallel} = 15.53$ ,  $\alpha_{\perp} = 11.82$ ,  $\beta_{\parallel} = 29.9$ ,  $\beta_{\perp} = 7.9$ .
- [37] K. F. Lee, D. M. Villeneuve, P. B. Corkum, and E. A. Shapiro, *Phys. Rev. Lett.* **93**, 233601 (2004).
- [38] U. Even, J. Jortner, D. Noy, N. Lavie, and C. Cossart-Magos, *J. Chem. Phys.* **112**, 8068 (2000).
- [39] M. J. J. Vrakking, *Rev. Sci. Instrum.* **72**, 4084 (2001).